The Mid-Infrared Spectra of Brown Dwarfs

D. Saumon[1], M. S. Marley[2] and K. Lodders[3]

ABSTRACT

We present an analysis of brown dwarf model spectra in the mid-infrared spectral region ($5 - 20\,\mu$m), in anticipation of data obtained with the Space Infrared Telescope Facility. The mid-infrared spectra of brown dwarfs are in several ways simpler than those in the near-infrared and yet provide powerful diagnostics of brown dwarf atmospheric physics and chemistry, especially when combined with ground-based data. We discuss the possibility of detection of new molecular species and of the silicate cloud, predict strong observational diagnostics for non-equilibrium chemistry between CO and CH_4, and N_2 and NH_3, and speculate on the possibility of discovering brown dwarf stratospheres.

Subject headings: stars: low mass, brown dwarfs — radiative transfer — molecular processes — infrared: stars

1. Introduction

The near-infrared and optical spectra of brown dwarfs have received intense observational and theoretical scrutiny (see the recent reviews by Basri 2000 and Burrows et al. 2001) but their mid-infrared spectra have been relatively neglected both in observation and theory. There are only two announced photometric detections of a brown dwarf beyond $5\,\mu$m (Matthews et al. 1996; Creech-Eakman et al. 2003) and neither strongly constrains models. Although synthetic mid-IR spectra have been published (e.g. Marley et al. 1996; Tsuji, Ohnaka & Aoki 1999; Allard et al. 2001; Burrows, Sudarsky & Lunine 2003) there has yet been no detailed discussion of the expected spectral diagnostics in L and T dwarfs. With the Space Infrared Telescope Facility (SIRTF) now in orbit, the dramatic improvement in

[1]Los Alamos National Laboratory, MS F699, Los Alamos, NM 87545

[2]NASA Ames Research Center, MS 245-5, Moffett Field, CA 94025

[3]Planetary Chemistry Laboratory, Department of Earth and Planetary Sciences, Washington University, St. Louis, MO 63130-4899

our ability to observe brown dwarfs in the mid-infrared will give new insights in the astrophysics of the complex atmospheres of these cool, dim denizens of our neighborhood. In this *Letter*, we present mid-IR model spectra of brown dwarfs and discuss their properties in terms of effective temperature, important molecular absorbers, the role of silicate clouds, and anticipate potential discoveries with SIRTF.

The instruments onboard SIRTF cover the wavelength range from 3 to $180\,\mu$m. Two of these will target brown dwarfs: the Infrared Array Camera (IRAC) and the Infrared Spectrograph (IRS). Brown dwarfs will be imaged by IRAC in four bandpasses centered at $3.6\,\mu$m, $4.5\,\mu$m, $5.8\,\mu$m, and $8.0\,\mu$m, respectively (Fig. 1)[4]. Since brown dwarfs become very dim and their spectra contain little information beyond $20\,\mu$m, the most useful IRS observations will be in the "Short wavelength, Low resolution" (SL) and the less sensitive "Short wavelength, High resolution" (SH) modes[5]. The SL and SH modes cover the 5.3 – $14.2\,\mu$m and the 10.0 – $19.5\,\mu$m spectral bands, respectively.

2.   Atmosphere models and spectra

To model the atmospheres and spectra of the L- and T-dwarfs we employ the radiative-convective equilibrium atmosphere model of Marley et al. (1996; further described in Burrows et al. 1997 and Marley et al. 2002) which includes the precipitating cloud model of Ackerman & Marley (2001). High resolution spectra are computed from the initial temperature profile and cloud structure (Saumon et al. 2000; Geballe et al. 2001). The chemistry is computed in the framework of the cloud condensation model (Lodders 1999a; Lodders & Fegley 2002; Lodders 2002; Lewis 1969). The opacity includes the molecular lines of H_2O, CH_4, CO, NH_3, H_2S, PH_3, TiO, VO, CrH, FeH, CO_2, HCN, C_2H_2, C_2H_4, C_2H_6 complemented with the atomic lines of the alkali metals (Li, Na, K, Rb and Cs) and continuum opacity sources from H_2 CIA, H_2, H and He Rayleigh scattering, H^- bf and ff, H_2^- ff, He^- ff, and H_2^+ bf and ff. While the chemical equilibrium is computed with a large number of condensates, only Fe, $MgSiO_3$, Al_2O_3, H_2O, and NH_3 are considered in the cloud model. Condensed Mg_2SiO_4 is accounted for with $MgSiO_3$ and the remaining condensates are not appreciable sources of opacity.

We consider spectra from $T_{\rm eff} = 600$ to $2400\,$K which covers the full range of L and T dwarfs. We limit the discussion to models with solar metallicity. The sedimentation

---

[4]`http://sirtf.caltech.edu/SSC/irac`

[5]`http://sirtf.caltech.edu/SSC/irs`

parameter of the cloud model is fixed at $f_{\mathrm{sed}} = 3$, which gives a good representation of far-red and near-IR photometry of L dwarfs (Marley et al. 2002; Burgasser et al. 2002) and of the ammonia cloud deck of Jupiter as well (Ackerman & Marley 2001). For simplicity, we do not take into account the possibility of cloud disruption near the L/T boundary (Burgasser et al. 2002).

3. Mid-infrared spectra of brown dwarfs

The combination of IRAC photometry and IRS spectroscopy with ground-based optical and near-IR data will give the complete spectral energy distributions (SED) of many brown dwarfs. Empirical bolometric corrections immediately follow as well as the bolometric luminosity for objects with known parallaxes. An independent determination of T_{eff} (e.g. by fitting spectra with models) will give the gravity, radius, and mass of individual brown dwarfs.

It is well known that in the far-red and near-IR, the brightness temperature T_{br} of brown dwarfs varies strongly with wavelength due to the high contrast between opacity windows and molecular absorption bands. This is still true in the mid-IR up to about $11\,\mu$m, thereafter T_{br} gradually decreases to stabilize at $\sim$75% of T_{eff} beyond $18\,\mu$m. Only near $6\,\mu$m and near $10\,\mu$m does T_{br} become as large as T_{eff}. For $4 \lesssim \log g\,(\mathrm{cgs}) \lesssim 5.5$, the pressure at the mid-IR photosphere stays between 0.1 and 3 bar, depending mostly on wavelength and surface gravity and least on T_{eff}. Basically, the mid-IR spectra of brown dwarfs are formed at $T \lesssim T_{\mathrm{eff}}$ and pressures of about 1 bar.

3.1. Molecular species

Figure 1 identifies the mid-IR molecular absorbers in a sequence of spectra from 600 to 2400 K. By far, the most important absorber is H_2O throughout the entire spectral range, except for two strong molecular bands due to CH_4 and NH_3. Beyond $15\,\mu$m, all features are due to H_2O, with the exception of a few weak NH_3 bands between 32 and $46\,\mu$m for models with $T_{\mathrm{eff}} \lesssim 800$ K. In the high-T_{eff} spectra, the fundamental band of CO at $4.8\,\mu$m and a weak TiO band at $10\,\mu$m are the only features not originating from H_2O. The step in the spectrum $\sim 6.5\,\mu$m is a H_2O feature. The TiO band disappears at 2200 K but the CO band persists down to 900 K in these cloudy models. As T_{eff} decreases, new molecular bands appear and steadily increase in strength. The $10.5\,\mu$m band of NH_3 appears at 1150 K. This band is very broad and dominates the spectrum from 8.5 to $16\,\mu$m at $T_{\mathrm{eff}} \leq 800$ K. Weaker bands of NH_3

appear at $900\,\mathrm{K}$ ($5.5 - 7\,\mu\mathrm{m}$) and $800\,\mathrm{K}$ ($3.9 - 4.5\,\mu\mathrm{m}$). The former is superimposed on a strong H_2O band, however. Methane shows only one band in the mid-IR, centered at $7.8\,\mu\mathrm{m}$. It appears at $1600\,\mathrm{K}$ and becomes very strong at low T_{eff} to dominate the spectrum between 7 and $9.2\,\mu\mathrm{m}$. Broad, featureless CIA opacity appears faintly in the 9 to $13\,\mu\mathrm{m}$ region in cool models below $1000\,\mathrm{K}$, but it shows no gravity sensitivity and is probably undetectable.

Our current phosphorus chemistry uses updates for several P-gases (PH, PH_3, PN, PS; Lodders 1999b, 2004) and the P_4O_6 gas thermodynamic properties from Gurvich, Veyts & Alcock (1989) instead of those from Chase (1998). Our previous models used P_4O_6 data from Chase (1998) and calculated spectra did not show the strongest PH_3 band centered at $4.3\,\mu\mathrm{m}$, just to the blue of the fundamental CO band. However, the Gurvich et al. data make P_4O_6 significantly less stable which results in a larger abundance of PH_3 and the band appears below $1100\,\mathrm{K}$ with a characteristic narrow absorption spike. This feature should provide a good observational test of the phosphorus chemistry in brown dwarfs, but its signature in IRAC band 2 photometry will have to be distinguished from possibly enhanced CO (Section 5).

The most abundant sulfur-bearing compound is H_2S, a molecule that has yet to be detected in brown dwarfs. Mid-IR observations will not improve its prospects of being noticed since its opacity is consistently $3 - 4$ orders of magnitude below that of H_2O.

We predict that CO and CH_4 will be visible simultaneously in the mid-IR for $T_{\mathrm{eff}} \lesssim 1600\,\mathrm{K}$, i.e. from mid-L to mid-T spectral types. The NH_3 band at $10.5\,\mu\mathrm{m}$ will be easy to detect and is a characteristic of all T dwarfs (see Section 5, however). Observations of Gl 229B should confirm the weak detection of this molecule in the near-IR (Saumon et al. 2000).

Figure 1 shows that the mid-IR spectra of brown dwarfs are characterized by molecular bands with strong T_{eff} dependences below $1600\,\mathrm{K}$. Fitting the IRS spectra alone with models should allow the determination of T_{eff} of brown dwarfs of mid-L and later spectral types.

3.2. Silicate cloud

The effects of silicate, iron, and corundum clouds on the near-IR spectra of brown dwarfs have been discussed extensively (Ackerman & Marley 2001; Allard et al. 2001; Burgasser et al. 2002; Cooper et al. 2003; Marley et al. 2002; Tsuji 2002; Tsuji & Nakajima 2003). Because the mid-IR photosphere is characterized by a fairly constant brightness temperature and a single dominant absorber (H_2O), the spectral signature of clouds stands out more clearly than in the near-IR. Most interesting is the possibility of detecting the silicate cloud

opacity feature $\sim 10\,\mu$m. Figure 2 shows spectra computed with and without the cloud opacity using the same cloudy atmospheric structure. We find that the silicate feature (a rise in the opacity between 9 and $10\,\mu$m to a new plateau) is masked by a similar behavior in the H_2O and CH_4 opacities. Nevertheless, the cloud opacity is large enough to appear in two windows where the gas is less opaque in models with $1200 \lesssim T_{\mathrm{eff}} \lesssim 2000\,$K: from ~ 4 to $6.5\,\mu$m (affecting IRAC bands 1 through 3) and from 9 to $13\,\mu$m. The effect is strongest at $T_{\mathrm{eff}} \sim 1600\,$K, which corresponds to the largest cloud optical depth above the $10\,\mu$m photosphere. Because the silicate absorption flattens the spectrum noticeably in the 9 to $12\,\mu$m range, its identification should be fairly straightforward in IRS spectra of mid-L dwarfs. For models with a higher condensate sedimentation efficiency ($f_{\mathrm{sed}} = 5$), the thinner cloud layer remains optically thin above the photosphere and is invisible at $10\,\mu$m. This feature can thus serve as a diagnostic of the vertical structure of the cloud model as its strength depends strongly on the cloud's vertical extent and on the particle size.

3.3.   IRAC colors of brown dwarfs

The IRAC will image brown dwarfs and provide photometry in 4 broad bandpasses (Fig. 1), labeled Band 1 through 4. Bands 1 and 2 cover wavelengths not accessible to the IRS.

As can be seen in Fig. 1, Band 2 covers the bands of CO and PH_3 but is nevertheless the least affected by strong molecular bands over the full range of T_{eff} of interest. Bands 1 and 4 are increasingly affected by CH_4 absorption below $T_{\mathrm{eff}} \sim 1500\,$K. Strong H_2O absorption appears in Band 3 below $T_{\mathrm{eff}} \sim 1200\,$K.

A study of color-color diagrams shows that IRAC colors will be most useful as diagnostics of brown dwarf physical properties for $T_{\mathrm{eff}} \lesssim 1400\,$K. At higher T_{eff}, the colors change little with T_{eff} or the T_{eff} and gravity dependences become hopelessly tangled. For brown dwarfs with known distances, color-magnitude diagrams provide a good discriminant of both T_{eff} and gravity.

4.   Trace molecular species

The IR spectra of giant planets reveal the presence of trace carbon species such as CO_2, C_2H_2, and HCN in *emission*. These arise primarily from the photochemistry of CH_4 (also seen in emission) in the stratosphere, i.e. above a temperature inversion in the atmosphere (Moses 2000). No published brown dwarf model shows a temperature inversion, mainly because the present knowledge of the physics of brown dwarf atmospheres is too primitive to

model a credible stratosphere. We nevertheless anticipate that brown dwarfs also may have stratospheres (Yelle 2000) and observations in the mid-IR are a powerful way to discover them by detecting emission features from trace molecules such as CO_2, C_2H_2, C_2H_4, C_2H_6, and HCN that should arise from photochemistry driven by the stratospheric and possibly the weak interstellar UV flux. In L and T dwarfs, H_2O remains in the gas phase and can participate in the photochemistry, leading to the formation of species such as HCO and CH_2O (Friedson, Wilson & Moses 2003).

In the absence of a stratosphere, these molecules would appear in *absorption*. The equilibrium abundances, i.e. in the absence of photochemistry, are all quite low. We have calculated the minimum enhancement factor (ϵ) of the abundance of several trace species required for detection. We define ϵ as the ratio of the column density of the trace species above the photosphere that is needed for detection to the equilibrium column density above the photosphere. For each species in Table 1, we give the wavelength of the strongest opacity feature, the T_{eff} that is most favorable for detection (i.e. giving the lowest enhancement factor), and the enhancement factor. Clearly, none of these species is likely to be detected in absorption, except for CO_2, which would be favored by higher metallicity and lower gravity. For instance, the equilibrium abundance of CO_2 should be marginally detectable at $15\,\mu m$ in a model with $T_{eff} = 1200\,K$ and $\log g = 4$.

Objects with masses below $13\,M_J$ do not burn deuterium and deuterated molecular species are expected in their atmospheres. With its distinctive $4.55\,\mu m$ band and a relatively large abundance, CH_3D is the most easily detected deuterated species expected in brown dwarfs. We find that for $CH_3D/CH_4 = 2 \times 10^{-5}$, an enhancement factor of $\gtrsim 250$ would be necessary to detect it in T dwarfs above $T_{eff} = 600\,K$ (Table 1). Detection becomes easier at lower T_{eff} but is very unlikely among the known objects.

5. Non-equilibrium chemistry

Vertical transport in brown dwarf atmospheres can lead to non-equilibrium abundances in slowly reacting species such as CO and N_2. The net effect is to enhance the upper atmosphere abundances of CO and N_2 to the detriment of CH_4, H_2O and NH_3 (Fegley & Lodders 1996; Griffith & Yelle 1999; Lodders & Fegley 2002). The detection of greatly enhanced CO (Noll, et al. 1997) and of depleted NH_3 (Saumon et al. 2000) in Gl 229B, as well as the M' flux deficiency observed in several T dwarfs (Golimowski et al. 2004) suggest that non-equilibrium chemistry is a general phenomenon in brown dwarfs. Nevertheless, it remains mostly unexplored observationally.

We have modeled the non-equilibrium spectra of brown dwarfs following the method described in Saumon et al (2003). We find that the $7.8\,\mu$m band of CH_4 appears at $T_{\text{eff}} \sim$ 1400 K and 1200 K for mixing coefficients of $K_{zz} = 10^2$ and $K_{zz} = 10^4\,\text{cm}^2/\text{s}$, respectively, compared to 1600 K in the case of equilibrium chemistry. The $10.5\,\mu$m band of NH_3 appears at $T_{\text{eff}} \lesssim 1000$ K for $K_{zz} \gtrsim 10^2\,\text{cm}^2/\text{s}$, instead of 1150 K. Because of the the relatively flat equilibrium abundance profile of NH_3, this result is nearly independent of K_{zz}. While NH_3 can be depleted by more than one order of magnitude (for $T_{\text{eff}} = 800$ K), the 10-11 μm features remain strong (Fig. 3).

6. Conclusions

Spectroscopy with the IRS instrument on SIRTF between 5 and 20 μm will complete the sampling of the spectral energy distribution of brown dwarfs. From our analysis of our mid-IR synthetic spectra, we find that the new data will: 1) clearly reveal the presence of NH_3 in T dwarfs, despite the strong depletion due to vertical transport in the atmosphere, 2) likely detect the silicate cloud $\sim 10\,\mu$m in mid-L dwarfs and put strong constraints on the vertical structure of the cloud, 3) lead to a much more complete picture of non-equilibrium chemistry among CO, CH_4, H_2O, N_2 and NH_3, 4) show CO_2 in low-gravity, high metallicity targets near the L/T transition, 5) *not* reveal interesting species such as H_2S, CH_3D, and the H_2 CIA opacity, and 6) possibly discover brown dwarf stratospheres through emission from trace species such as CO_2, HCN, HCO, C_2H_2, C_2H_4, C_2H_6 and CH_2O. Furthermore, we predict that: 7) a strong band of PH_3 at $4.3\,\mu$m falls in the IRAC band 2, 8) IRAC photometry will be most useful for objects below 1400 K, and 9) photospheric spectra of brown dwarfs are of very little interest beyond 20 μm. The mid-IR spectral window is rich in diagnostics of brown dwarf atmospheres. Our understanding of these cool neighbors will grow dramatically with our first mid-IR observations with SIRTF.

REFERENCES

Ackerman, A. & Marley, M. S. 2001, ApJ, 556 872

Allard, F., Hauschildt, P. H., Alexander, D. R., Tamanai, A., & Schweitzer, A. 2001, ApJ, 556, 357

Basri, G. 2000, ARA&A, 38, 485

Burgasser, A. J., Marley, M. S., Ackerman, A. S., Saumon, D., Lodders, K., Dahn, C. C., Harris, H. C., & Kirkpatrick, J. D. 2002, ApJ, 571, L151

Burrows, A., Hubbard, W. B., Lunine, J. I. & Liebert, J. 2001, Rev. Mod. Phys., 73, 719

Burrows, A., Marley, M. S., Hubbard, W. B., Lunine, J. I., Guillot, T., Saumon, D., Freedman, R. S., Sudarsky, D. & Sharp, C. 1997, ApJ, 491, 856

Burrows, A., Sudarsky, D. & Lunine, J. I. 2003, `astro-ph/0304226`

Chase, M.W. 1998, NIST-JANAF Thermochemical Tables, 4th ed., J. Phys. Chem. Ref. Data Monogr. 9.

Cooper, C. S., Sudarsky, D., Milsom, J. A., Lunine, J. I. & Burrows, A. 2003, ApJ, 586, 1320

Creech-Eakman, M., Serabyn, E., Orton, G. S., & Hayward, T. L. 2003, IAU Symposium, 211, 421

Fegley, B. Jr. & Lodders, K. 1996, ApJ, 472, L37

Friedson, A. J., Wilson, E. & Moses, J. I. 2003, BAAS, 35, 944

Geballe, T. R., Saumon, D., Leggett, S. K., Knapp, G. R., Marley, M. S. & Lodders, K. 2001, ApJ, 556, 373

Golimowski, D. A. et al. 2004, in preparation

Griffith, C. A. & Yelle, R. V. 1999, ApJ, 519, L85

Gurvich, L.V., Veyts, I.V., & Alcock, C. B. 1989, Thermodynamic properties of individual substances, 4th ed. (Hemisphere Publ. Co., New York)

Lodders, K. 1999a, ApJ, 519, 793

Lodders, K. 1999b, J. Phys. Chem. Ref. Data, 28, 1705

Lodders, K. 2002, ApJ, 557, 974

Lodders, K. 2004, J. Phys. Chem. Ref. Data, 33, in press

Lodders, K. & Fegley, B. Jr. 2002, Icarus, 155, 393.

Marley, M. S., Saumon, D., Guillot, T., Freedman, R. S., Hubbard, W. B., Burrows, A., & Lunine, J. I. 1996, Science, 272, 1919

Marley, M. S., Seager, S., Saumon, D., Lodders, K., Ackerman, A. S., Freedman, R. S. & Fan, X. 2002, ApJ, 568, 335

Matthews, K., Nakajima, T., Kulkarni, S., & Oppenheimer, B. R. 1996 , AJ, 112, 1678

Moses, J. I. 2000, in From Giant Planets to Cool Stars, ASP Conf. Series Vol 212, C. A. Griffith & M. S. Marley, Eds. (ASP: San Francisco), 196.

Noll, K. S., Geballe, T. R. & Marley, M. S. 1997, ApJ, 489, L87

Saumon, D., Geballe, T. R., Leggett, S. K., Marley, M. S., Freedman, R. S., Lodders, K., Fegley, B., & Sengupta, S. K. 2000, ApJ, 541, 374

Saumon, D., Marley, M. S., Lodders, K. & Freedman, R. S. 2003 in Brown Dwarfs, IAU Symposium 211, ed. E. L. Martín (San Francisco: ASP), 345

Tsuji, T. 2002, ApJ, 575, 264

Tsuji, T., Ohnaka, K. & Aoki, W. 1999, ApJ, 520, L119

Tsuji, T. & Nakajima, T. 2003, ApJ, 585, L151

Yelle, R. V., 2000, in From Giant Planets to Cool Stars, ASP Conf. Series Vol 212, C. A. Griffith & M. S. Marley, Eds. (ASP: San Francisco), 267.

Fig. 1.— Sequence of mid-IR spectra of brown dwarfs with T_{eff} ranging from 600 to 2400 K (from bottom to top) in steps of 200 K. All models have solar metallicity, $\log g = 5$, $f_{\text{sed}} = 3$ and are shown at a spectral resolution of 200. Spectra are shifted vertically for clarity. Molecular bands that appear at high T_{eff} are identified at the top, those that appear at low T_{eff} are shown at the bottom. Outside of those bands, H_2O is responsible for all features. Weak bands are indicated with dashed lines. The bandpasses of the four IRAC filters are shown by thick solid lines at the top.

Fig. 2.— Effect of silicate cloud opacity on the mid-IR spectra of brown dwarfs. The spectra shown have $T_{\text{eff}} = 1000$ to 2400 K in steps of 200 K. The dotted lines show spectra computed from the same cloudy (T, P) structures and chemistry, but without the cloud opacity. IRAC bands 3 and 4 are shown by thick solid lines at the top.

Fig. 3.— Effect of non-equilibrium chemistry on the mid-IR NH_3 band. The spectra shown have $T_{\text{eff}} = 800$ to 1600 K in steps of 200 K. The spectra shown are computed computed from the same cloudy (T, P) structures but with equilibrium (solid) and non-equilibrium (dotted) chemistry. See Fig. 2 for details.
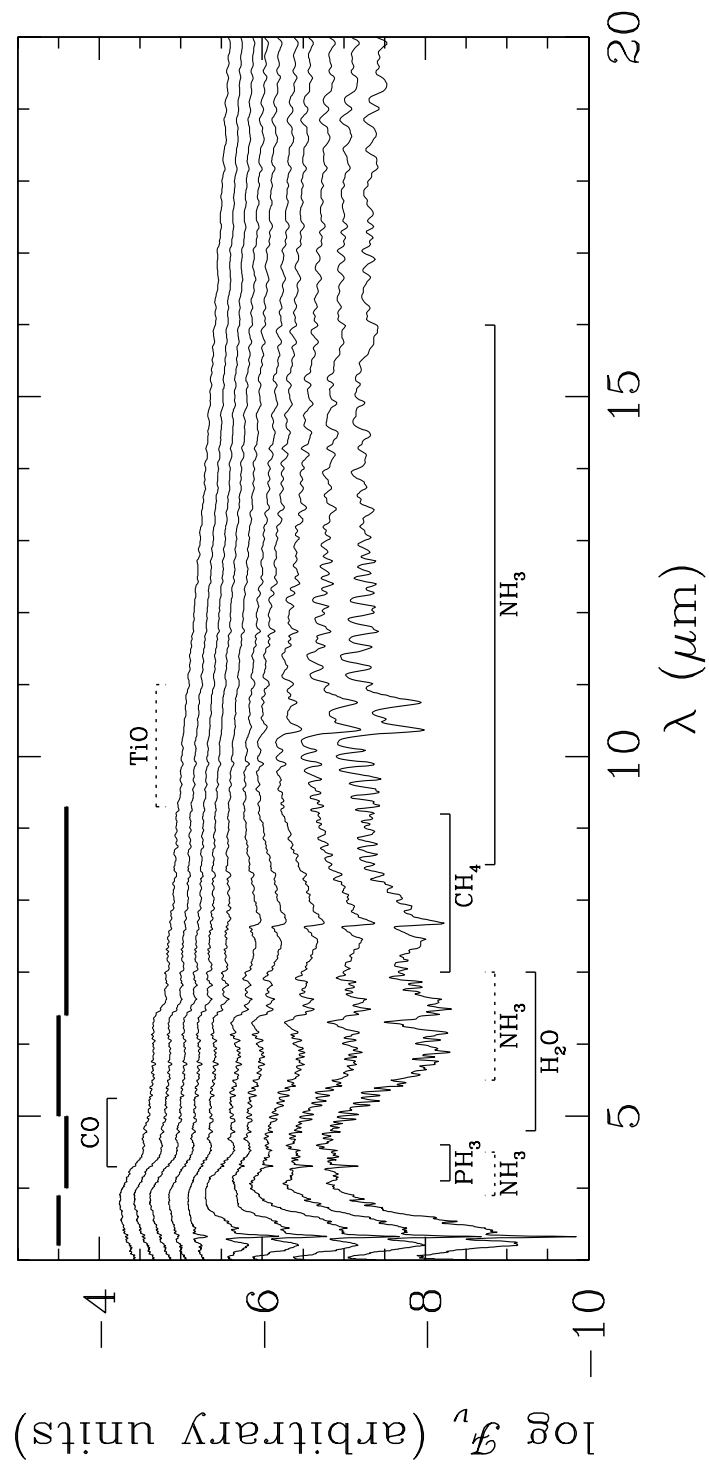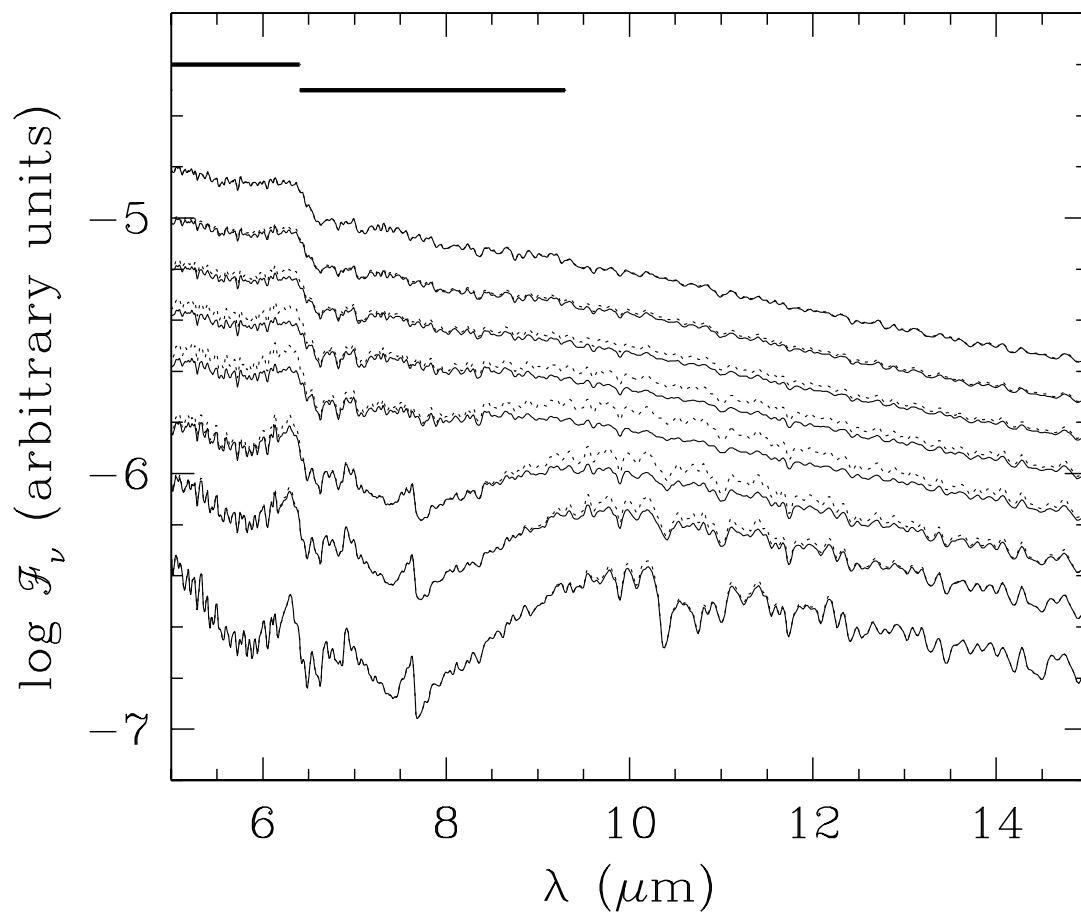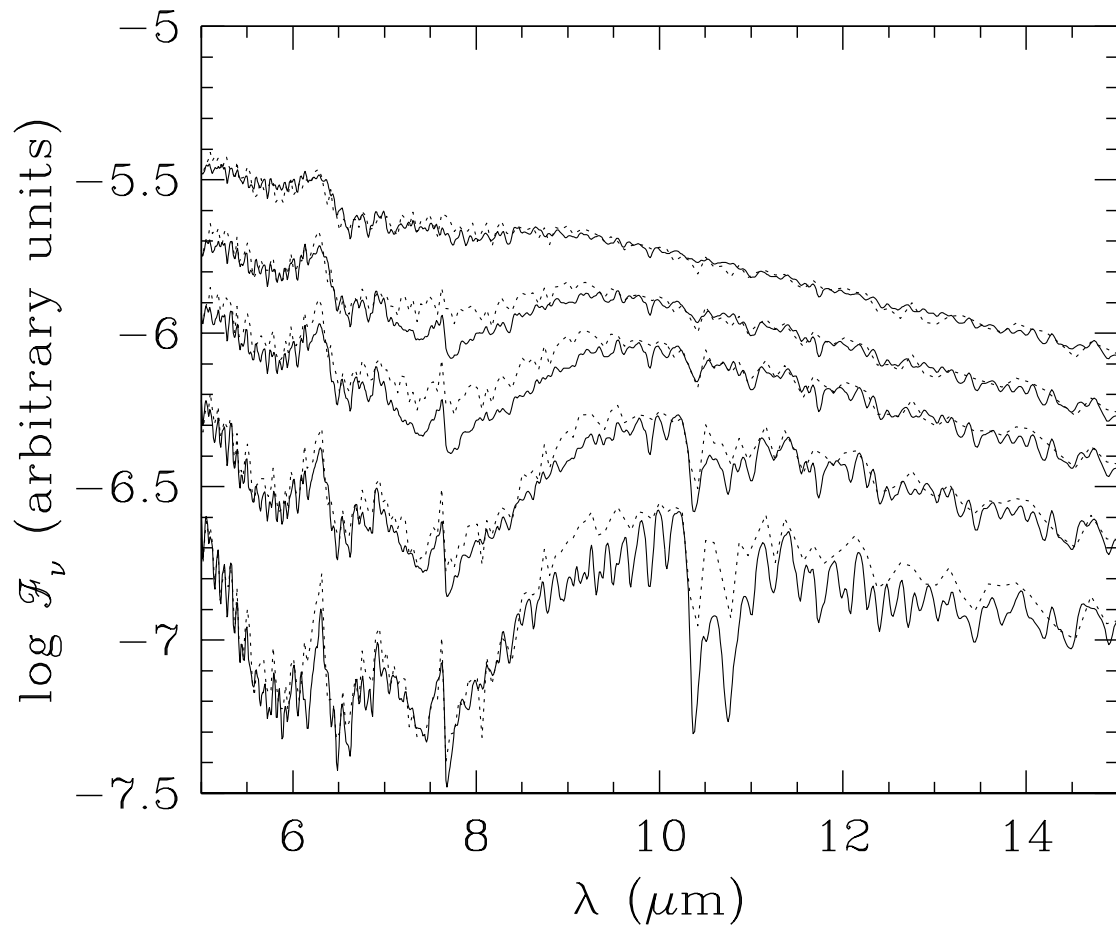
Table 1.   Enhancement factors for trace species.[a]

Species	$\lambda(\mu\mathrm{m})$	T_{eff} (K)	$\log(\epsilon)$
CO_2	15.0	1400	0.7
HCN	14.0	1400	2.7
C_2H_2	13.7	1400	5.8
C_2H_4	10.5	1200	4.9
C_2H_6	~ 12.2	1000	3.5
CH_3D	4.55	< 600	< 2.4[b]

[a]For $\log g = 5$ and solar metallicity.

[b]Cloudless atmosphere model.